Enhanced Frequency Response From Industrial Heating Loads for Electric Power Systems

Yue Zhou, *Member, IEEE*, Meng Cheng, and Jianzhong Wu, *Member, IEEE*

***Abstract*—Increasing penetration of renewable generation results in lower inertia of electric power systems. To maintain the system frequency, system operators have been designing innovative frequency response products. Enhanced frequency response (EFR) newly introduced in the UK is an example with higher technical requirements and customized specifications for assets with energy storage capability. In this paper, a method was proposed to estimate the EFR capacity of a population of industrial heating loads, bitumen tanks, and a decentralized control scheme was devised to enable them to deliver EFR. Case study was conducted using real UK frequency data and practical tank parameters. Results showed that bitumen tanks delivered high-quality service when providing service-1-type EFR, but underperformed for service-2-type EFR with much narrower deadband. Bitumen tanks performed well in both high- and low-frequency scenarios, and had better performance with significantly larger numbers of tanks or in months with higher power system inertia.**

***Index Terms*—Bitumen tanks, decentralized control, enhanced frequency response (EFR), industrial heating loads.**

I. Introduction

FREQUENCY is an indicator of the real-time balance between supply and demand of an electric power system, and is also an important aspect of power quality that affects the power usage of all the customers. In the process of low-carbon transition due to environmental concerns, many countries have been witnessing increasing penetration of renewable generation and decreasing capacity of conventional synchronous generators in their generation mix. This fact results in lower power system inertia, and hence makes it even difficult to maintain the system frequency within the required range.

As a result, power system operators in many countries have been investigating innovative frequency response products. For example, the Italian transmission system operator (TSO) trialed frequency containment reserve and synthetic rotational inertia to obtain fast acting response proportional to the frequency deviation and the rate of change of frequency (ROCOF) [1]. PJM in the US designed Regulation D (RegD) product for devices with high ramp rate but limited energy supply capability [2]. In Ireland, fast frequency response (FFR) was designed to provide faster response than the existing primary operating reserve [3].

In the UK, National Grid Electricity Transmission (NGET), the TSO of Great Britain (GB), created an innovative frequency response product, enhanced frequency response (EFR), in 2016, with higher technical requirements and customized specifications for assets with energy storage capability [4]. EFR sets a deadband in which the active power output of EFR assets is allowed to vary within a $\pm 9\%$ range, so that the response capability of the assets is able to be managed and recovered. Moreover, EFR specifies higher technical requirements on response speed (within 1 s), accuracy and ramp rate. These distinct features make EFR be one of the leading frequency response products in the world [5].

Since 2017, several studies have been made on using battery energy storage systems (BESSs) to provide EFR. A control algorithm was devised in [6] to provide EFR considering all the technical requirements of EFR. Triad avoidance was conducted at the same time, and the control was verified by a real 2 MW/1 MW·h lithium–titanate type BESS. Provision of EFR from BESSs was also evaluated by real-time network simulation and power hardware in the loop in [5]. Energy arbitrage was considered along with EFR provision in [7]. EFR from both BESSs and hybrid energy storage systems was studied in [8]. Energy exchange and battery cycling aging were evaluated. In [9], EFR was generalized, simulated, and assessed in the Continental Europe System. In [10], EFR was compared to traditional firm frequency response (FFR) services in the UK, and some EFR specifications were examined. With these studies, it is shown that BESSs are able to provide EFR well, even with other services provided at the same time.

Besides BESSs, thermostatically controlled loads (TCLs) are the major category of flexible demand that has the potential to provide EFR due to their thermal storage capability. All types of TCLs, including residential, commercial, and industrial TCLs, are candidates. There have been extensive studies made to explore demand response from TCLs, including arbitrage in energy markets [11] and provision of various ancillary services such as renewable generation following [12], peak shaving [13],

Manuscript received July 21, 2018; revised October 6, 2018; accepted October 27, 2018. Date of publication November 9, 2018; date of current version June 12, 2019. This work was supported in part by the Engineering and Physical Sciences Research Council Supergen Hub on Energy Networks Project and in part by the FLEXIS Project which is part-funded by the European Regional Development Fund through the Welsh Government. Information about the data underpinning the results presented here, including how to access them, can be found in the Cardiff University data catalogue at http://doi.org/10.17035/d.2018.0064005779. Paper no. TII-18-1894. *(Corresponding author: Jianzhong Wu.)*

The authors are with the School of Engineering, Cardiff University, Cardiff CF24 3AA, U.K. (e-mail: ZhouY68@cardiff.ac.uk; chengm89@qq.com; WuJ5@cardiff.ac.uk).

Color versions of one or more of the figures in this paper are available online at http://ieeexplore.ieee.org.

Digital Object Identifier 10.1109/TII.2018.2879907

voltage support [14], network loss reduction [15], frequency control and reserves [16], [17].

For frequency response, in terms of residential TCLs, authors in [18] and [19] investigated the potential and developed design considerations and parameter selection for residential air conditioners to provide load following and secondary frequency control services. Authors in [20] and [21] evaluated economic and environmental benefits of residential refrigerators that provide primary frequency control services in the future GB power system. Kondoh *et al.* [22] evaluated the potential of residential electric water heaters to provide secondary frequency control services. For commercial buildings, the heating, ventilation and air conditioning systems attract increasing attention recently. The electrical load of air handling units was modulated to provide secondary frequency control services in three different ways: fan speed offset [23]–[25], supply pressure/mass flow setpoint offset [25], [26], and thermostat setpoint offset [27], [28]. A comprehensive review has been conducted in [29].

Industrial heating loads are also important candidates that contribute to frequency control of electric power systems due to their large power consumption and high automation level. For decades, industrial heating loads such as those in steelworks have been participating in underfrequency load shedding schemes, where they are set to be disconnected automatically at a predefined low frequency. Recently, some studies have been conducted to enable industrial heating loads to provide dynamic frequency response services. For example, a control algorithm was devised for bitumen tanks for the GB power system [30]. Similar methodology was applied to melting pots that smelt aluminum [31].

In this paper, a novel contribution was made to enable industrial heating loads to provide EFR that has different and higher technical requirements compared with the conventional frequency response services. Also, performance evaluation was conducted in practical context. Specifically, bitumen tanks were studied as a representative. The main work of this paper is presented as follows.

1) A method was proposed to estimate how much capacity a population of bitumen tanks can provide for EFR.
2) A decentralized control scheme was devised to enable the tanks to provide EFR.
3) For EFR from bitumen tanks, technical and economic performances were evaluated using real UK frequency data and real tank parameters from field tests.

Compared to the existing studies focusing on utilizing residential [18]–[22] or commercial TCLs [23]–[29] to provide conventional frequency response services, this paper focuses on utilizing industrial heating loads, which have similar but different thermal features and parameters, to provide EFR service, which is an innovative frequency response product in the UK with unique technical requirements and remuneration mechanism.

Compared to the existing studies using industrial heating loads to provide conventional frequency response service [30], [31], this paper is a comprehensive extension to enable and evaluate industrial heating loads to provide the innovative EFR service, which is of concrete significance in practice. To achieve this, this paper has made three major contributions: 1) a method was proposed to estimate the capacity of a group of industrial heating loads to provide EFR; 2) new control rules have been developed to fit the requirements of EFR, specifically, the setting of trigger frequencies considers the delivery envelope and symmetry requirements specified in EFR, based on the EFR capacity estimated, as detailed in Section III-C2; and 3) economic evaluation from the market perspective (i.e., the remuneration assessment based on the technical performance and the remuneration rules) was conducted.

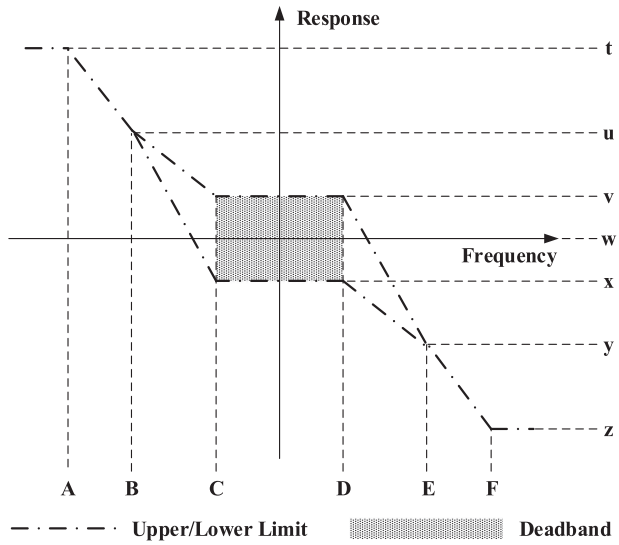

Fig. 1. EFR delivery envelope [4].

II. Technical Specifications and Evaluation Metrics of EFR

EFR was designed by NGET as an alternative solution to procuring larger volumes of existing frequency response products to improve management of system frequency in both prefault and postfault situations. NGET issued detailed technical specifications and evaluation metrics for EFR [4].

A. Technical Specifications

The technical specifications for EFR are divided into five aspects: delivery envelope, ramp rate, speed, duration, and symmetry.

1) Delivery Envelope: The delivery envelope specifies the area in which the response of EFR assets should lie, as shown in Fig. 1 [4].

In Fig. 1, upper and lower limits of the response at different frequencies are illustrated. It is seen that there is a deadband (the gray zone) in which the response is allowed to vary in a wide range, which is designed for EFR assets to recover their response capability. Outside the deadband, the allowable band specified by the upper and the lower limits gradually shrinks and finally collapses into a single line when the frequency deviation is large (in both overfrequency and underfrequency directions).

EFR is divided into two different types of services when the knee points of the delivery envelope take different values, as presented in Table I [4]. Note that in Table I, the response is normalized as a percentage of the contracted capacity. The key

TABLE I
PARAMETERS OF EFR DELIVERY ENVELOPE [4]

Frequency	Service 1 (Hz)	Service 2 (Hz)	Response	Service 1 (%)	Service 2 (%)
A	49.5	49.5	t	100	100
B	49.75	49.75	u	44.44444	48.45361
C	49.95	49.985	v	9	9
D	50.05	50.015	w	0	0
E	50.25	50.25	x	-9	-9
F	50.5	50.5	y	-44.44444	-48.45361
			z	-100	-100

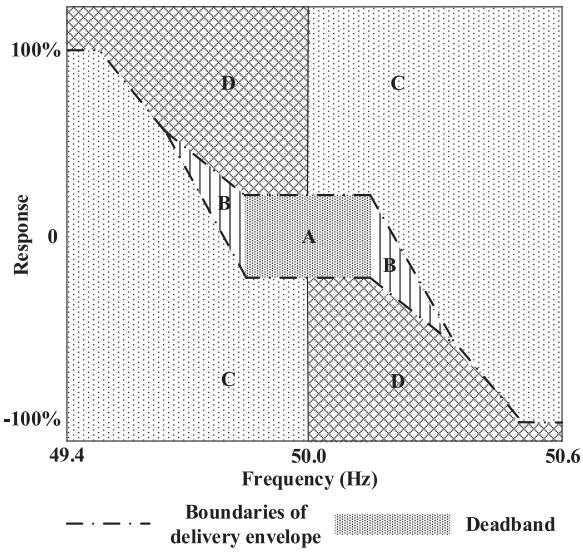

Fig. 2. Zone division for ramp rate constraints for EFR [4].

TABLE II
RAMP RATE CONSTRAINTS FOR EFR [4]

Zone	Constraints of the rate of change of response, *ROCOR*	
A	$-0.01 \le ROCOR \le 0.01$	(1)
B	$-\frac{1}{k}\cdot\frac{df}{dt}-0.01 \le ROCOR \le -\frac{1}{k}\cdot\frac{df}{dt}+0.01$	(2)
C	$-0.1 \le ROCOR \le 0.1$	(3)
D	$-2 \le ROCOR \le 2$	(4)

difference between the two services lies in that service-2-type EFR has a much narrower deadband, which imposes a higher technical requirement on EFR assets.

2) Ramp Rate Constraints: EFR assets also need to satisfy the constraints on ramp rates (i.e., the rate of change of response) to avoid the possible short-term stability problems, considering EFR is much quicker than the conventional frequency response [5].

The ramp rate constraints vary with the system frequency and the response provided at certain time point. Specifically, the status of EFR assets is divided into four zones, as illustrated in Fig. 2, with different constraints on ramp rates, as presented in Table II [4]. The ROCOR values in Table II are normalized by the contracted capacity per second.

Note that in (2) for Zone B, k takes different values for different types of EFR. For service-1-type EFR, k equals to 0.45, while for service-2-type EFR, k equals to 0.485. df/dt is the ROCOF.

Also note that the delivery envelope always takes precedence over the constraints on ramp rates whenever they contradict each other.

3) Response Speed: Response speed is measured by the time delay between the frequency deviation and response delivery. EFR requires this time to be no greater than 1 s [4]. The requirement is significantly higher than that of the conventional primary response in the UK, which requires the response to be delivered within 10 s [32].

4) Response Duration: EFR assets are required to have the capability to provide 100% contracted capacity (in both overfrequency and underfrequency directions) continuously for at least 15 min. Note that storage facilities (e.g., BESS) are exempted from providing EFR for a period of time after providing 15-min service with full capacity (this period called "extended frequency event"), but this kind of exemption is not applicable for flexible demand that provides EFR [4].

5) Symmetry: The contracted capacity of EFR assets in overfrequency and underfrequency directions is required to be the same [4].

B. Evaluation Metrics

NGET defined two indexes, service performance measure (SPM) and availability factor (AF), to measure the provision of EFR from technical and economic perspectives, respectively.

1) SPM: SPM is a normalized index calculated per settlement period (half an hour, i.e., 1800 s, in the UK) to reflect the delivery level of EFR. To define SPM, second-by-second performance measure (SBSPM) is first defined to quantify the service delivery for 1 s [4]

$$\text{SBSPM} = \begin{cases} 1 & R^{\text{lower}} - \varepsilon \le R \le R^{\text{upper}} + \varepsilon \\ \max\left(1 - \left|R - R^{\text{upper}}\right|, 0\right) & R > R^{\text{upper}} + \varepsilon \\ \max\left(1 - \left|R - R^{\text{lower}}\right|, 0\right) & R < R^{\text{lower}} - \varepsilon \end{cases} \tag{5}$$

where R^{lower} and R^{upper} are the lower and the upper limits of the response at the second, as detailed in Fig. 1 and Table I; ε is the accuracy threshold, being 0.01; R is the normalized response actually provided by the EFR assets, calculating as

$$R = \frac{\dot{R}}{C} \tag{6}$$

where $\dot{R}$ (kW) is the actual response at the second before normalization, and C (kW) is the contracted EFR capacity.

From (5), it is seen that SBSPM ranges from "0" to "1," with larger values representing better performance. When the actual response is within the delivery envelope, SBSPM takes the best value, "1." When the actual response goes out of the upper or lower limit, SBSPM is reduced according to the magnitude of deviation from the upper or the lower limits.

TABLE III
DEFINITION OF AF FOR EFR [4]

Service Performance Measure	Availability Factor
SPM < 50%	0%
50% ≤ SPM < 75%	50%
75% ≤ SPM < 95%	75%
SPM ≥ 95%	100%

Based on SBSPM, SPM is calculated as the average of SBSPM over a settlement period (1800 s) [4]

$$\mathrm{SPM} = \frac{\sum_{s\in \boldsymbol{S}} \mathrm{SBSPM}_s}{1800} \tag{7}$$

where $\boldsymbol{S}$ is the set of all the seconds in the settlement period, and s is the index of a second.

Furthermore, annual service performance measure is calculated as the average of SPM over a rolling 12-month period [4]

$$\mathrm{ASPM}_j = \frac{\sum_{j\in \boldsymbol{J}} \mathrm{SPM}_j}{|\boldsymbol{J}|} \tag{8}$$

where $\boldsymbol{J}$ is the set of all the settlement periods in the 12 months considered, and j is the index of a settlement period.

If APSM <95%, NGET will look to discuss the underperformance with the EFR provider with a view to identifying underlying causes and mitigation measures (thus in this paper, the "95%" is called as "underperformance limit"). If APSM <50%, the EFR contract will be terminated by NGET (hence, the "50%" is called as "termination limit").

2) AF: AF is defined based on SPM to decide the proportion of remuneration that the EFR provider can obtain for each settlement period, as detailed in Table III.

For example, if SPM ≥95%, the EFR provider is able to obtain 100% contracted remuneration for that settlement period, but if 75% ≤ SPM <95%, only 75% remuneration can be obtained.

III. EFR FROM BITUMEN TANKS

This section details how bitumen tanks, as a representative of industrial heating loads, provide EFR. First of all, bitumen tanks and their modeling are briefly described. Then, a method for estimating the EFR capacity of a population of tanks is proposed. Finally, a decentralized control scheme is devised for the tanks to provide EFR.

A. Modeling of Bitumen Tanks

Bitumen tanks are well-insulated tanks for storing liquid bitumen that is required to be stored within a certain temperature range. Conventionally, hysteresis control is used to control the electric heater of a tank, and the resulting temperature dynamics are illustrated in Fig. 3. It is observed that the temperature increases when the heater remains ON, while decreases due to stand-by heat loss when the heater is OFF. The heater turns OFF when the temperature reaches the upper limit, while turns ON when it reaches the lower limit.

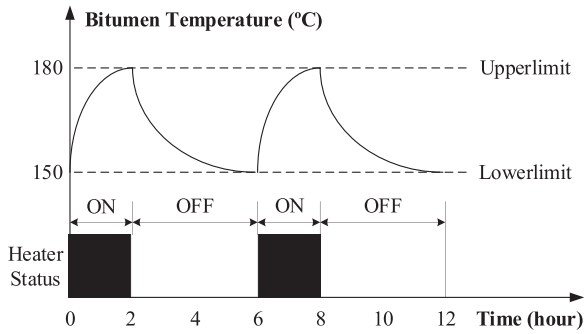

Fig. 3. Thermodynamics and heater ON/OFF status of a bitumen tank.

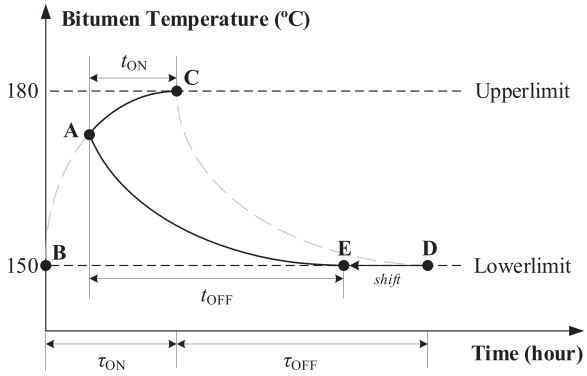

Fig. 4. Diagram of t_{ON} and t_{OFF} at some temperature of a bitumen tank [30].

The evolving thermodynamics of a tank are able to be modeled by an ON–OFF time model [30]. As shown in Fig. 4, in the ON–OFF time model, the state of a tank, i.e., any temperature point between the upper and the lower temperature limits (e.g., Point A in Fig. 4), is mapped to a pair of variables $\langle t_{ON},\ t_{OFF}\rangle$. t_{ON} is defined as the time needed from the current temperature point to the upper limit if the heater keeps ON (Curve AC in Fig. 4). Similarly, t_{OFF} is defined as the time needed from the current temperature point to the lower limit if the heater keeps OFF (Curve AE in Fig. 4).

In the ON–OFF time model, a tank is characterized by its ON and OFF periods, marked as τ_{ON} and τ_{OFF}. The ON period, τ_{ON}, is defined as the time needed from the lower limit to the upper limit if the heater keeps ON (Curve BC in Fig. 4). Similarly, the OFF period, τ_{OFF}, is defined as the time needed from the upper limit to the lower limit if the heater keeps OFF (Curve CD in Fig. 4). According to the field test data [30], typical ON periods range from 42 to 180 min, and typical OFF periods range from 60 to 480 min.

With the above definitions, the relationship between t_{ON} and t_{OFF} of a tank, which is characterized by τ_{ON} and τ_{OFF}, is able to be expressed as follows:

$$t_{ON} = \tau_{ON} \cdot \sqrt{1 - \left(\frac{t_{OFF}}{\tau_{OFF}}\right)^2} \tag{9}$$

$$t_{OFF} = \tau_{OFF} \cdot \sqrt{1 - \left(\frac{t_{ON}}{\tau_{ON}}\right)^2}. \tag{10}$$

TABLE IV
MODELING OF DYNAMIC STATE EVOLVEMENT OF A TANK

Heater Status		State Evolvement Expression	
t	$t+\Delta t$		
ON	ON	$t_{\mathrm{ON}}(t+\Delta t)=t_{\mathrm{ON}}(t)-\Delta t$	(11)
OFF		$t_{\mathrm{OFF}}(t+\Delta t)=\tau_{\mathrm{OFF}}\cdot\sqrt{1-[(t_{\mathrm{ON}}(t)-\Delta t)/\tau_{\mathrm{ON}}]^2}$	(12)
ON	OFF	$t_{\mathrm{ON}}(t+\Delta t)=\tau_{\mathrm{ON}}\cdot\sqrt{1-[(t_{\mathrm{OFF}}(t)-\Delta t)/\tau_{\mathrm{OFF}}]^2}$	(13)
OFF		$t_{\mathrm{OFF}}(t+\Delta t)=t_{\mathrm{OFF}}(t)-\Delta t$	(14)

As detailed in [30], (9) and (10) were obtained from the physical thermodynamic model of bitumen tanks and verified by practical field tests. Based on the physical thermodynamic model, a large number of $\langle t_{\mathrm{ON}},\ t_{\mathrm{OFF}}\rangle$ pairs were generated, corresponding to the different bitumen temperature points. Then, the curve fitting tool "cftool" in MATLAB was used to obtain the semicircle relationship between t_{ON} and t_{OFF} as described by (9) and (10). Then, practical field tests were conducted using two 40-kW and two 25-kW tanks. t_{ON} and t_{OFF} were measured at different temperatures of the tanks. It was shown that the $\langle t_{\mathrm{ON}},\ t_{\mathrm{OFF}}\rangle$ pairs generated by (9) and (10) matched closely with the measured ones, indicating that (9) and (10) can describe the thermodynamics of bitumen tanks very well.

Based on (9) and (10), the dynamic state evolvement of a tank, i.e., the relationship between the state at a time step t, $\langle t_{\mathrm{ON},t},\ t_{\mathrm{OFF},t}\rangle$, and the state at the next time step $t+\Delta t$, $\langle t_{\mathrm{ON},t+\Delta t},\ t_{\mathrm{OFF},t+\Delta t}\rangle$, is able to be described by the formulas in Table IV, given different heater status. Note that for the simulation regarding frequency response, the length of time steps, Δt, is usually taken from tens of milliseconds to 1 s. For example, in the case study section of this paper, for Cases 1 and 3–6 focusing on general technical and economic performance, 1 s was chosen, while for Case 2 exploring the time delay, a much shorter time step was used, being 10 ms.

With the state evolvement expression in Table IV, the hysteresis control applied to a tank is able to be described as follows: 1) if $t_{\mathrm{ON},t}$ decreases to 0, the heater turns OFF at the next time step $t+\Delta t$; and 2) if $t_{\mathrm{OFF},t}$ decreases to 0, the heater turns ON at the next time step $t+\Delta t$.

The model described in this section was used to simulate the bitumen tanks for the evaluation presented in Section IV of this paper.

B. Estimation of EFR Capacity for a Population of Tanks

Before being able to provide EFR, an EFR provider needs to submit the capacity (i.e., maximum amount of response) it can deliver in a tender to NGET. Once the tender is accepted, NGET contracts with the EFR provider, who then needs to provide the response that is proportional to the frequency deviation and the contracted capacity as shown in Fig. 1. Therefore, the EFR capacity of a population of tanks needs to be estimated beforehand.

1) Baseline Estimation: The response of a tank population, $\dot{R}$ (kW), is calculated as the difference between a pre-estimated baseline and the actual value of the active power consumption of the population

$$\dot{R}=\bar{P}-\sum_{i\in\boldsymbol{I}}P_i\cdot\mu_i \tag{15}$$

where $\bar{P}$ represents the baseline of the tank population. $\boldsymbol{I}$ represents the set of the tanks and i is the index of a tank. P represents the rated power of the heater of a tank. μ represents the actual ON/OFF status of the heater of a tank.

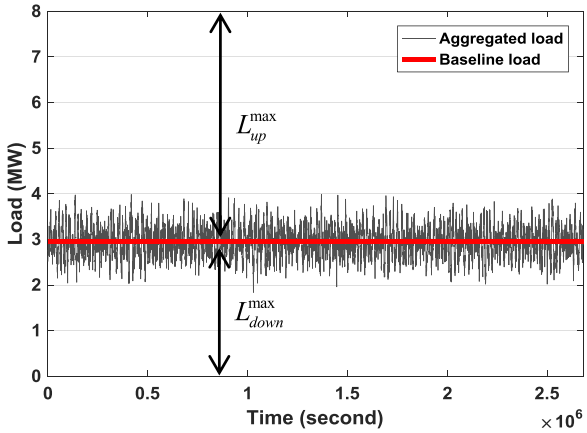

Fig. 5. Example of aggregated load of a population of 200 tanks over one month.

In practice, the tanks are highly heterogeneous, because of the diversity in a variety of tank parameters (e.g., the power rating of heaters, tank sizes, thermal insulation materials) and operational environments (e.g., properties of the bitumen stored and ambient air temperature). As a result, the aggregated load of a population of tanks, when not providing any frequency response, is usually stabilized at a certain level with some variations, as illustrated in Fig. 5.

Considering that the uncertainties are numerous and some of them are constantly changing, it is difficult to forecast the baseline in real time without delicate measurement and communication facilities. Therefore, in this paper, the baseline load of the tank population is simply estimated as the mean value of the historical aggregated load throughout a period of time during which the tanks did not provide any frequency response service

$$\bar{P}=\frac{\sum_{t\in\boldsymbol{T}}\sum_{i\in\boldsymbol{I}}P_i\cdot\mu_{i,t}}{|\boldsymbol{T}|} \tag{16}$$

where $\boldsymbol{T}$ represents the set of the time steps within the time window considered, and t is the index of a time step. Note that the length of the time window considered for baseline estimation should be comparable to the service time window during which the assets tender to provide EFR, usually ranging from one month to several months, and up to 48 months for EFR [4].

In practice, the baseline load of a tank population will not vary significantly at different times of a year. The reason is that, according to the physical thermodynamic model of tanks as detailed in [30], the electric power consumption of a tank is closely related to the heat loss which is the product of the overall heat transfer coefficient of the tank ($\mathrm{W\cdot m^{-2}\cdot K^{-1}}$), the surface area of the tank ($\mathrm{m^2}$), and the difference between bitumen temperature

in tank and ambient temperature (°C). Bitumen tanks are well insulated, and thus the overall heat transfer coefficient is very small. Furthermore, considering that the bitumen temperature is very high (normally 150–180 °C), the temperature difference between bitumen and ambient temperature is large and thus will not change a lot in percentage with the change of the ambient temperature. As a result, the variation of ambient temperature will not significantly affect the heat loss and thus will not significantly affect the power consumption. This conclusion has been supported by practical field tests conducted for a population of 76 bitumen tanks in the UK, showing that the variation of ambient temperature will not cause large variation for the electric load of the tank population [33].

2) EFR Capacity Estimation: Based on the baseline estimated, the EFR capacity of the tank population is able to be estimated. First of all, the maximum load increase potential of the tank population is calculated as

$$L_{\text{up}}^{\max} = \sum_{i \in \boldsymbol{I}} P_i - \bar{P} \tag{17}$$

while the maximum load reduction potential is just equal to the baseline load

$$L_{\text{down}}^{\max} = \bar{P}. \tag{18}$$

Then, considering the symmetry requirement of EFR (as presented in Section II-A5), the EFR capacity of the tank population should be

$$C = \min\left\{L_{\text{down}}^{\max}, L_{\text{up}}^{\max}\right\}. \tag{19}$$

In practice, for bitumen tanks, the OFF period, τ_{OFF}, is much longer than the ON period, τ_{ON}, so $L_{\text{down}}^{\max}$ is smaller than $L_{\text{up}}^{\max}$. As a result, (19) can be simplified as

$$C = L_{\text{down}}^{\max} = \bar{P}. \tag{20}$$

It can be seen that for a specific population of tanks, the EFR capacity is decided by its baseline load. As detailed in Section III-B1, the baseline may change, but will not vary significantly at different times of a year. Therefore, the EFR capacity may also change, but will not vary significantly throughout a year as well. Furthermore, even though there is some variation for baselines and thus EFR capacity in different seasons of a year, this does not matter a lot, because it is allowed to tender different EFR capacity for different months. Different baselines, which can be estimated based on the historical data of the same months in the past years, can be used to decide the EFR capacity tendered for different months.

C. Decentralized Control for Providing EFR

After submitting the EFR capacity to NGET, the tanks need to provide the corresponding EFR in real time according to the frequency deviation. A decentralized control scheme is devised to achieve this purpose, as illustrated in Fig. 6.

As shown in Fig. 6, the decentralized control scheme is applied to each bitumen tank and takes only local measurement of system frequency and bitumen temperature as input. The scheme is composed of a temperature control module, a frequency control module, and a coordination logic that integrates the output

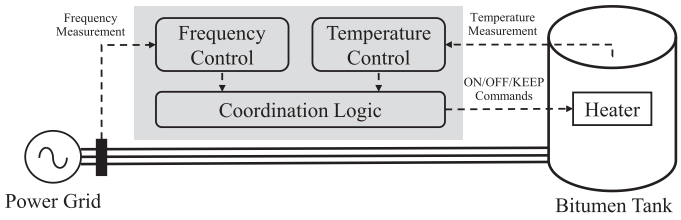

Fig. 6. Decentralized control scheme of a tank for the provision of EFR.

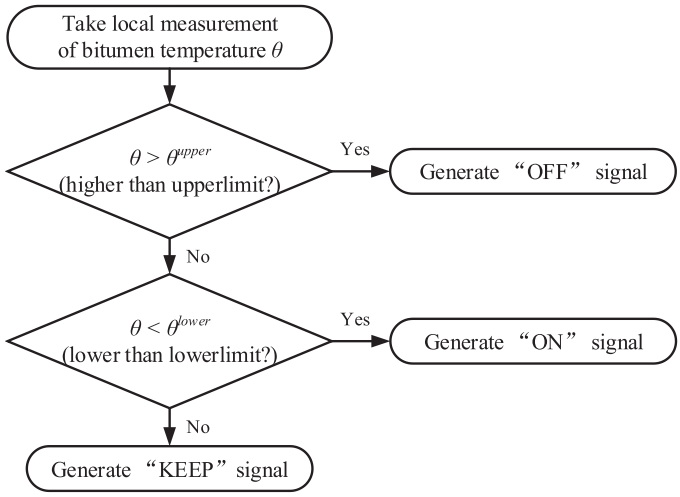

Fig. 7. Flowchart of the hysteresis temperature control.

signals from the previous two modules. The components are detailed as below.

1) Temperature Control: The hysteresis control of a tank, as described in Section III-A, is kept in the proposed scheme to guarantee the primary function (i.e., bitumen storage) of the tanks. The control takes local measurement of bitumen temperature as the input, and generates three types of output signals (i.e., "ON", "OFF," and "KEEP"). The "ON" and "OFF" signals mean to turn the heater of the tank ON and OFF, respectively, while the "KEEP" signal means to keep the heater status unchanged. The control logic is summarized in Fig. 7.

2) Frequency Control: An additional frequency control is applied to each tank for providing EFR. The control takes local measurement of system frequency as the input, and also generates three types of output signals ("ON," "OFF," and "KEEP"). A pair of trigger frequencies, f_{ON} and f_{OFF}, are assigned in the control. If the measured frequency, f, is lower than the trigger-OFF frequency, f_{OFF}, the "OFF" signal is generated, while the "ON" signal is generated if f is higher than the trigger-ON frequency f_{ON}. If f lies between f_{ON} and f_{OFF}, the "KEEP" signal is generated. This control logic is illustrated in Fig. 8.

In order to deliver the service that satisfies the EFR specifications, the trigger frequencies, f_{ON} and f_{OFF}, are preset in delicate ways. The f_{OFF} of each tank is randomly sampled from the interval $[f_A, f_C)$ that follows uniform distribution, where f_A and f_C are the frequencies at Points A and C in Fig. 1, with f_A being 49.5 Hz and f_C being 49.95 Hz (service-1-type) or 49.985 Hz (service-2-type). With this setting for each tank, the

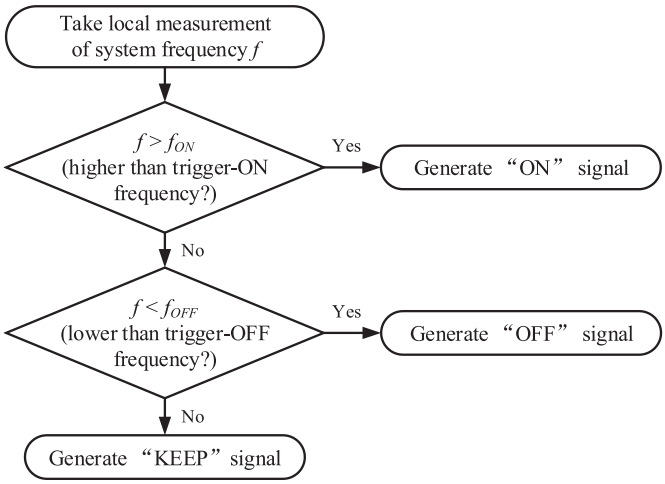

Fig. 8. Flowchart of the proposed frequency control.

following performance is achieved from the perspective of the whole tank population.

1) When the system frequency f is within $[f_C, 50]$, no tank is triggered to be turned OFF because $f > f_{\mathrm{OFF}}$ for any tank. This is consistent with the EFR specification that no response is required to be provided within the deadband as specified in Fig. 1.
2) When the system frequency f keeps decreasing below f_C, an increasing number of tanks are triggered to be turned OFF accordingly, because the trigger-OFF frequencies of the tanks are evenly distributed in $[f_A, f_C)$. In this way, underfrequency response (i.e., load reduction) is delivered proportional to the frequency deviation as specified in Fig. 1.

The trigger-ON frequencies, f_{ON}, are preset in the similar way, except that only a portion of tanks in the population should respond to overfrequency events because the EFR capacity of the population is smaller than the maximum load increase potential of the population (as previously presented in Section III-B). Therefore, the trigger-ON frequencies of a portion of the tanks (the proportion being $(1 - L_{\mathrm{down}}^{\max}/L_{\mathrm{up}}^{\max}) \times 100\%$) are preset as a number higher than f_F (50.5 Hz as shown in Fig. 1) so that those tanks will always not be triggered to be turned ON. The trigger-ON frequencies of the rest of the tanks in the population are randomly sampled from $(f_D, f_F]$ (as specified in Fig. 1 and Table I). In this way, overfrequency response (i.e., load increase) is able to be delivered, proportional to the frequency deviation and the contracted EFR capacity.

It is worth noting that the trigger frequencies for all the tanks can be updated locally and periodically (e.g., one week, one month, etc.) to ensure all the tanks have equal responsibility for providing EFR. The update should be conducted when the system frequency is within the deadband to avoid affecting the provision of EFR.

3) Coordination Logic: The coordination logic takes the signals from the temperature control and frequency control modules as the input and output the final command that decides the status of the heater. The final command also includes three types: "ON," "OFF," and "KEEP."

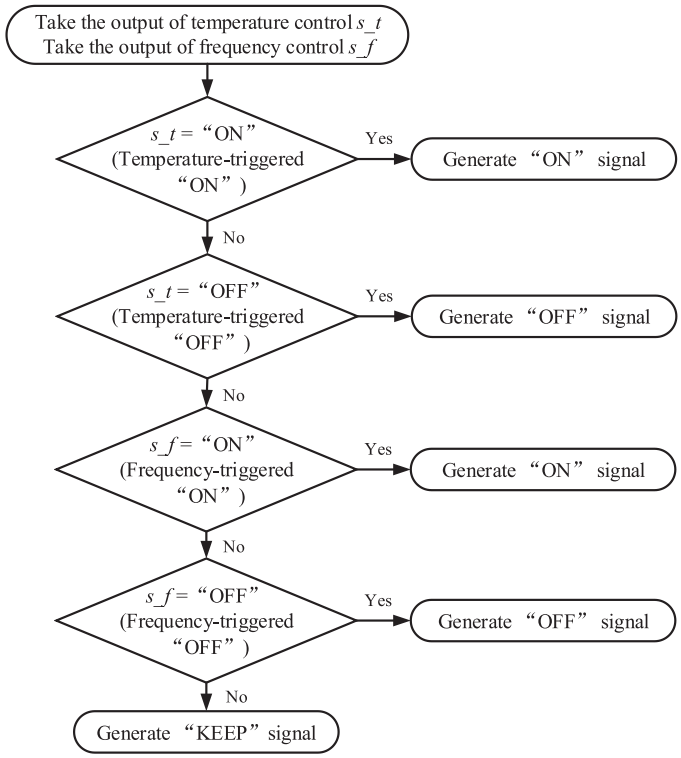

Fig. 9. Flowchart of the proposed coordination logic.

TABLE V
TYPICAL VALUES OF PARAMETERS OF BITUMEN TANKS [30]

Parameters	Range of Values
Rated Power	17 – 75 kW
ON Period	42 – 180 minutes
OFF Period	60 – 480 minutes

The principle of coordination is that the temperature control takes precedence over the frequency control anytime the temperature control outputs "ON" or "OFF" signals. Only when the temperature control outputs "KEEP" signals, the heater status is decided by the output of frequency control. This principle is to guarantee the primary function of the tanks and to avoid safety issues, e.g., the bitumen temperature far exceeds the upper limit. The detailed coordination logic is presented in Fig. 9.

IV. EVALUATION RESULTS

The performance of EFR service from bitumen tanks using the proposed capacity estimation method and decentralized control was evaluated based on real frequency data of the UK and tank parameters from real field tests conducted by Open Energi (a commercial aggregator in the UK). The second-by-second frequency data of the GB electric power system in 2016 was used [34]. The tank parameters were randomly sampled from the ranges as presented in Table V [30].

The total time for frequency measurement, frequency trigger and heater action of a tank follows a Gaussian distribution with the mean value being 0.7 s and standard deviation being 0.3125 s. This data come from a real field test conducted by Open Energi.

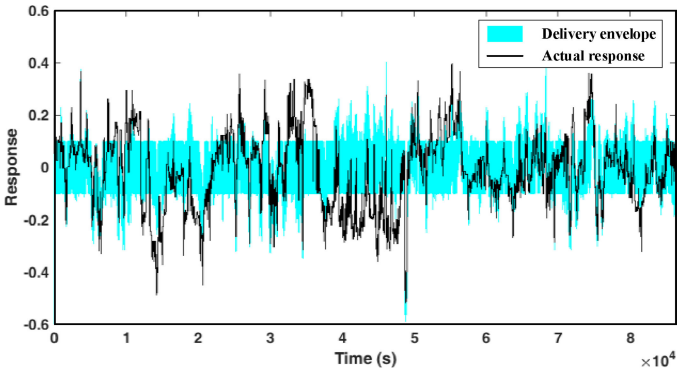

Fig. 10. Normalized response of the tank population in Case 1.

In the simulation, the time delay of each tank was randomly sampled from this Gaussian distribution.

Six cases were conducted in total. Case 1 is the base case that evaluated the technical and economic performance of EFR from the tanks. Case 2 studied the response speed (i.e., time delay of the response). Cases 3, 4, and 5 evaluated the impact of service types, frequency deviation, and size of the tank population, respectively. Case 6 verified the performance over long periods of time, i.e., two months with the highest and lowest system inertia of the year.

Note that the impact of the location of bitumen tanks was not evaluated in the case study, because the location has little impact on the performance of EFR. According to the technical specifications and evaluation metrics issued by NGET regarding EFR [4], when examining the performance of EFR, the actual response and the delivery envelope are calculated based on the active power and system frequency locally measured by on-site monitoring equipment of the EFR assets, i.e., bitumen tanks in this case (referring to [4, Appendix 7]). Furthermore, even if bitumen tanks at different site locations are aggregated to provide EFR, they are seen as a notional "aggregated facility," for which the aggregated response is the aggregation of the response locally measured at the individual tank subgroups at different locations (referring to [4, Appendixes 3 and 4]). That is to say, even if the frequencies are different at different locations of the power system (note that the differences are usually neglectable), the bitumen tanks only have the obligation to respond to the frequency locally measured. Therefore, the location of bitumen tanks has little impact on the performance of EFR, so in this paper, the location factors were not considered in the design of the method and not evaluated in the case study.

A. Case 1: Base Case

Sevice-1-type EFR from a population of 200 tanks was evaluated in a day with the highest system frequency in 2016 (16 November 2016). The time step of simulation was 1 s. The response was illustrated in Fig. 10.

In Fig. 10, the second-by-second response of the tank population (the black line), normalized by the contracted capacity, is illustrated with the allowable response range (the teal zone). If the response lies in the teal zone, it means that the response lies within the delivery envelope, thus satisfying the requirement. On the other hand, if the response lies outside the teal zone (i.e., within the white zones), it means that the response violates the delivery envelope at that time point. It is seen from Fig. 10 that the response varied with the system frequency deviation and lied within the delivery envelope most of the time throughout the day.

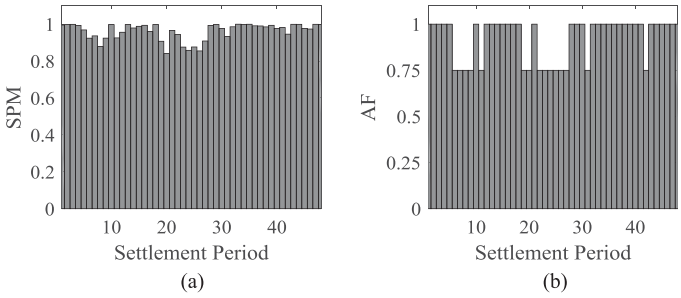

Fig. 11. SPM and AF for Case 1. (a) SPM. (b) AF.

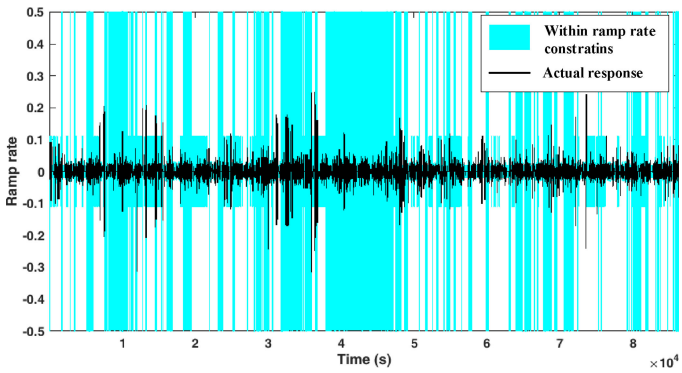

Fig. 12. Normalized ramp rates of the tank population in Case 1.

To further quantify the response quality and assess its impact on the remuneration, the scores of SPM and AF were calculated as shown in Fig. 11. From Fig. 11(a), it is seen that the SPM was generally at a high level, with the minimum SPM being 0.8401. It is further calculated that the average SPM throughout the day was 0.9613, which is higher than both the underperformance limit (95%) and termination limit (50%) specified by NGET, showing that the performance of EFR from the tanks is qualified in this sense. From Fig. 11(b), it is seen that the AFs were 0.75 or 1.00 throughout the day and the average AF was 0.9219, indicating that the tank population could obtain 92.19% of the contracted remuneration.

The actual and allowable ramp rates across the day are shown in Fig. 12. Similar to Fig. 10, the teal zones represent the allowable ramp rates while the outside white zones represent that the ramp rates violate the requirement. It is seen that most of the time the ramp rates were within the constraints across the day except for a few cases. NGET has not issued any quantified penalty guidelines for the violation of ramp rate constraints.

B. Case 2: Study of Response Speed

All the settings of this case were kept the same as those of Case 1 except that the simulation time step was chosen as a much smaller value, 10 ms, for assessing the response speed. Besides, instead of simulating the whole day, only the settlement period containing the highest frequency of the year (13:30–14:00) was

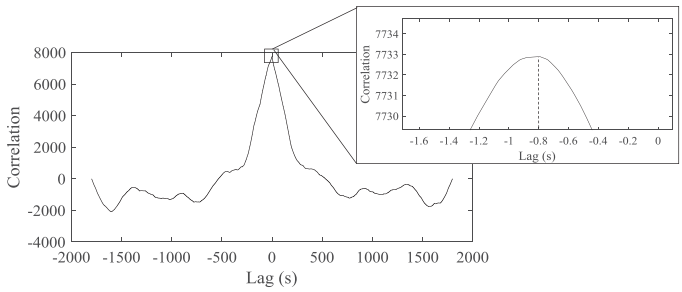

Fig. 13. Cross correlation between the expected and actual response.

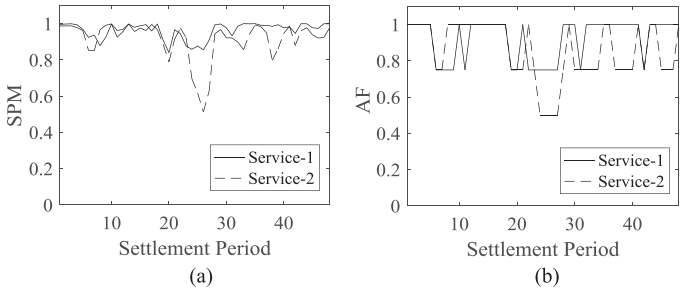

Fig. 14. SPM and AF when providing different types of EFR. (a) SPM. (b) AF.

studied in this case, due to the short time step and the resulting high computational burden.

A cross-correlation analysis between the expected response (the average values of the upper and lower limits of the response envelope in Fig. 1) and actual response was conducted. The results are shown in Fig. 13.

It is seen that the maximum correlation happened with a lag of –0.8 s, implying that the time delay of EFR from the tank population was 0.8 s, which satisfies the EFR specification on response speed (less than 1 s).

C. Case 3: Study of Service Types

All the settings of this case were kept the same as those of Case 1 except that the tanks were assumed to provide service-2-type EFR, for assessing the impact of service types. The SPM and AF for providing service-2-type EFR are illustrated in Fig. 14, together with the results of service-1-type EFR from Case 1.

It is seen that generally the SPM and AF for service-2-type EFR were worse than those for service-1-type EFR, because of the much narrower deadband. The average SPM of service-2-type EFR is 0.9130, which has already been lower than the underperformance limit, although still much higher than the termination limit. The average AF was 0.8542, which was 7.34% lower than that of service-1-type EFR.

D. Case 4: Study of Frequency Deviation Types

All the settings of this case were kept the same as those of Case 1 except that the tanks were assumed to provide EFR in a day with the lowest frequency in 2016 (20 November 2016), for assessing the impact of frequency deviation types. The average SPM and AF were presented in Table VI, together with results of Case 1 for comparison.

TABLE VI
AVERAGE SPM AND AF FOR HIGH-FREQUENCY AND LOW-FREQUENCY DAYS

Day Type	Average SPM	Average AF
High-Frequency	0.9613	0.9219
Low-Frequency	0.9760	0.9583

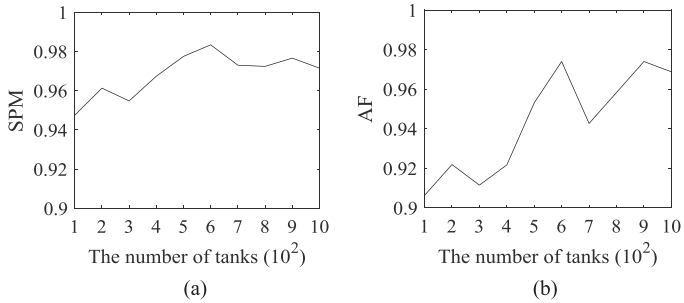

Fig. 15. Average SPM and AF with different sizes of tank populations providing EFR. (a) Average SPM. (b) Average AF.

It is seen that for both days the average SPM was higher than the underperformance limit. Generally, the performance for the two days was quite close to each other.

E. Case 5: Study of Tank Population Size

All the settings of this case were kept the same as those of Case 1 except that the tank populations with different sizes were assumed to provide EFR, for assessing the impact of size of the tank population. The results are illustrated in Fig. 15.

It is seen that generally a larger number of tanks (e.g., 500–1000) resulted in higher SPM and AF scores than a smaller number of tanks (e.g., 100–500). However, if the numbers of tanks are close (e.g., 200 and 300, or 600 and 700 in Fig. 15), larger numbers of tanks did not necessarily result in better performance. Overall speaking, the SPM was always higher than the underperformance limit and the AF was always higher than 0.9 (which means that more than 90% of contracted remuneration could be obtained) for the tank populations with their sizes ranging from 100 to 1000, when providing service-1-type EFR.

F. Case 6: Evaluation Over Longer Periods of Time

All the aforementioned sections evaluated the performance over two extreme days of the year to have a close look at how the service was provided and what the performance is like. In this section, longer periods of time were used for evaluation to obtain more robust results. Specifically, two months, January and July of 2016, have been selected to conduct the simulation, considering that they are the months with highest and lowest inertia of the year for the GB power system. Note that all the other settings are kept the same as those of Case 1.

Both the technical and economic performance (measured by SPM and AF) have been evaluated for both service-1-type and service-2-type EFR in January and July. The SPM and AF for each settlement period are shown from Figs. 16 to 19, and the average SPM and AF are presented in Table VII.

Comparing the results with different service types (i.e., comparing Figs. 16 and 17 for January, as well as Figs. 18 and

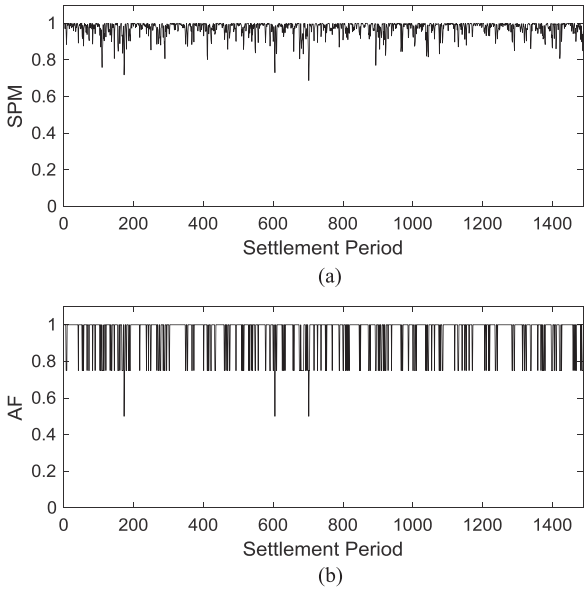

Fig. 16. SPM and AF for service-1-type EFR in January. (a) SPM. (b) AF.

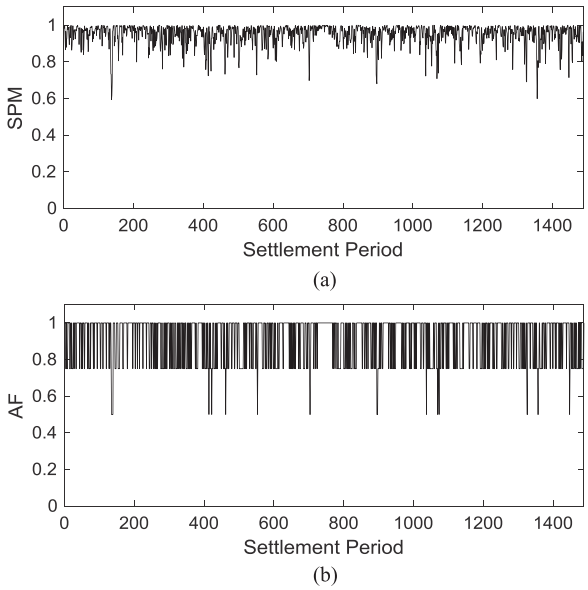

Fig. 17. SPM and AF for service-2-type EFR in January. (a) SPM. (b) AF.

19 for July), it is observed that for many settlement periods, the SPM and AF of service-2-type EFR were lower than those of service-1-type EFR for both January and July. In terms of the average performance as presented in Table VII, the average SPM and AF of service-2-type EFR were about 5% lower than those of service-1-type EFR in both January and July, and were both lower than the underperformance limit specified for EFR. This conclusion is consistent with the one drawn in Section IV-C which was conducted given an extreme day of the year.

Comparing the results in different months (i.e., comparing Figs. 16 and 18 for service-1-type EFR, as well as Figs. 17 and 19 for service-2-type EFR), it is seen that for many settlement

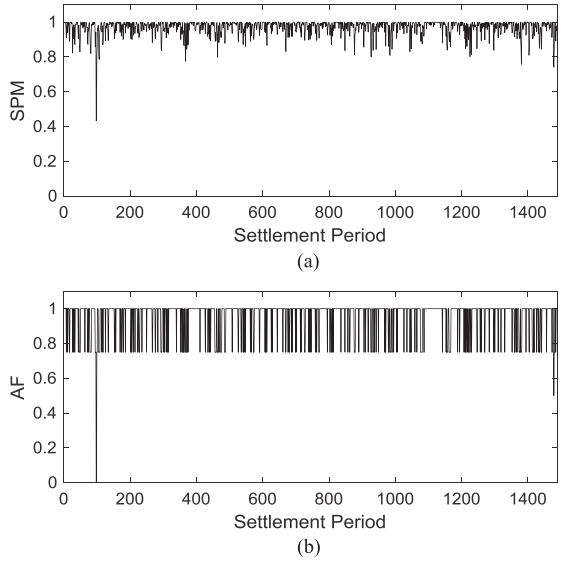

Fig. 18. SPM and AF for service-1-type EFR in July. (a) SPM. (b) AF.

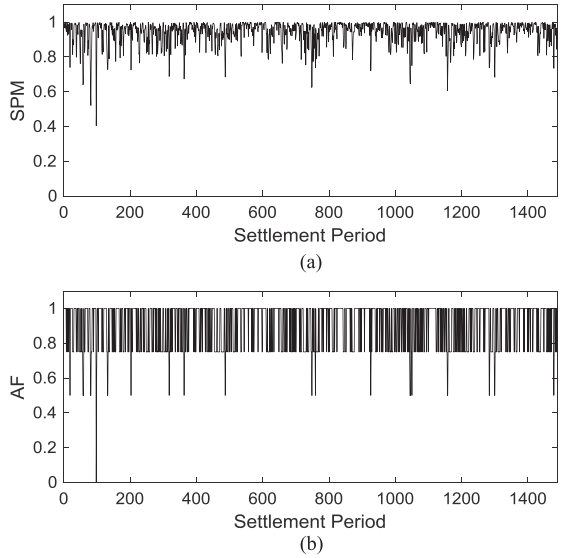

Fig. 19. SPM and AF for service-2-type EFR in July. (a) SPM. (b) AF.

TABLE VII
AVERAGE SPM AND AF FOR DIFFERENT SERVICE TYPES IN JANUARY AND JULY

Month	Service Type	Average SPM	Average AF
January	1	0.9726	0.9553
	2	0.9496	0.9071
July	1	0.9694	0.9471
	2	0.9425	0.8980

periods, the SPM and AF in January were higher than those in July. In terms of the average performance as presented in Table VII, the average SPM and AF in January were slightly (around 1%) higher than those in July. This is because in January the power system inertia was higher than that in July, having resulted in less severe fluctuation in system frequency.

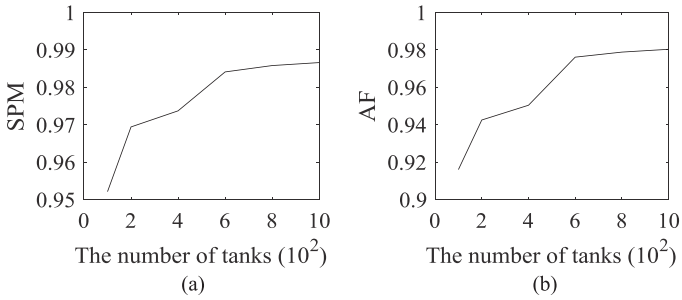

Fig. 20. Average SPM and AF with different sizes of tank populations providing EFR (one-month results). (a) SPM. (b) AF.

The impact of the tank population size on the EFR performance was also verified by one-month simulation (service-1-type EFR in July was chosen). The results are illustrated in Fig. 20. It is seen that with the increasing number of tanks in the population, the EFR performance got better, which is consistent with the results in Section IV-E which was conducted given an extreme day of the year.

V. Conclusion

This paper studied using industrial heating loads to provide novel frequency response service with more complex and strict technical requirements. Bitumen tanks and EFR in the UK were studied as representatives. A method was proposed to estimate the EFR capacity of a population of bitumen tanks, and a decentralized control scheme was devised to enable the tanks to deliver EFR service.

The performance of EFR service from bitumen tanks was evaluated using real system frequency data of the UK and tank parameters from field tests. Simulation results in the day with the highest frequency of the year showed that when providing service-1-type EFR, bitumen tanks satisfied all the technical specifications including underperformance limit, termination limit, and response speed, except some minor violation for ramp rate constraints. Over 90% of contracted remuneration could be obtained. However, when providing service-2-type EFR, the underperformance limit was violated. Simulation results in the day with the lowest frequency of the year showed that bitumen tanks performed well in both high-frequency and low-frequency scenarios. Moreover, it was revealed that better performance could be achieved with significantly larger numbers of tanks. Simulation over longer periods of time (months) confirmed the conclusions that higher performance could be provided for service-1-type EFR than that for service-2-type EFR, and the performance would be better with an increasing number of tanks in the population. Besides, it was revealed that the performance would be better in the months with higher power system inertia.

Regarding the applicability, this paper took bitumen tanks as a representative to be studied, but the proposed method can be applied to other industrial heating loads such as melting pots in aluminum and steel making processes, which are important industrial loads in many countries and consume a large amount of electric energy. Possible concrete examples refer to the many practical case studies conducted by Open Energi (although they are now providing conventional frequency response services rather than EFR), including various industrial heating loads in asphalt plants, building material manufacturing plants, aluminum gravity die casting plants, etc. [35]. However, it is also worth noting that although other industrial heating loads may share very similar thermal characteristics with bitumen tanks, the specific values of thermal parameters may be significantly different (e.g., 715–755 °C for melting pots, which is much higher than 150–180 °C for bitumen tanks), so the technical and economic evaluation need to be reconducted using the proposed method for other industrial heating loads to reveal their capability to provide EFR.

References

[1] R. Benato, G. Bruno, F. Palone, R. M. Polito, and M. Rebolini, "Large-scale electrochemical energy storage in high voltage grids: Overview of the Italian experience," *Energies*, vol. 10, no. 1, pp. 1–17, 2017.

[2] T. K. Chau, S. S. Yu, T. Fernando, and H. H. Iu, "Demand-side regulation provision from industrial loads integrated with solar PV panels and energy storage system for ancillary service," *IEEE Trans. Ind. Informat.*, vol. 14, no. 11, pp. 5038–5049, Nov. 2018.

[3] *SEM-13-098 DS3 System Services Technical Definitions—Decision Paper*, SEM Committee, Jun. 2018. [Online]. Available: https://www.semcommittee.com/sites/semcommittee.com/files/media-files/SEM-13-098%20%20DS3%20System%20Services%20Technical%20Definitions%20Decision%20Paper%20-%20FINAL_0.pdf

[4] *Enhanced Frequency Response—Invitation to Tender for Pre-qualified Parties v2.2*, Nat. Grid plc, Jun. 2018. [Online]. Available: https://www.nationalgrid.com/sites/default/files/documents/Enhanced%20Frequency%20Response%20ITT%20v2_2%20clean.pdf

[5] D. M. Greenwood, K. Y. Lim, C. Patsios, P. F. Lyons, Y. S. Lim, and P. C. Taylor, "Frequency response services designed for energy storage," *Appl. Energy*, vol. 203, pp. 115–127, 2017.

[6] B. Gundogdu, S. Nejad, D. T. Gladwin, M. P. Foster, and D. A. Stone, "A battery energy management strategy for UK enhanced frequency response and triad avoidance," *IEEE Trans. Ind. Electron.*, vol. 65, no. 12, pp. 9509–9517, Dec. 2018, doi: 10.1109/TIE.2018.2818642.

[7] B. Gundogdu, D. T. Gladwin, and D. A. Stone, "Battery SOC management strategy for enhanced frequency response and day-ahead energy scheduling of BESS for energy arbitrage," in *Proc. 43rd Annu. Conf. IEEE Ind. Electron. Soc.*, Beijing, China, Oct. 2017, pp. 7635–7640.

[8] M. Bahloul and S. K. Khadem, "Design and control of energy storage system for enhanced frequency response grid service," in *Proc. IEEE Int. Conf. Ind. Technol.*, Lyon, France, Feb. 2018, pp. 1189–1194.

[9] S. Canevese, D. Cirio, A. Gatti, M. Rapizza, E. Micolano, and L. Pellegrino, "Simulation of enhanced frequency response by battery storage systems: The UK versus the Continent Europe system," in *Proc. IEEE Int. Conf. Environ. Elect. Eng. IEEE Ind. Commer. Power Syst. Eur.*, Milan, Italy, Jun. 2017, pp. 1–6.

[10] A. Cooke, K. Forkasiewicz, and D. Strickland, "Energy storage for enhanced frequency response services," in *Proc. Int. Univ. Power Eng. Conf.*, Heraklion, Greece, Aug. 2017, pp. 1–6.

[11] J. Mathieu, M. Kamgarpour, J. Lygeros, G. Andersson, and D. Callaway, "Arbitraging intraday wholesale energy market prices with aggregations of thermostatic loads," *IEEE Trans. Power Syst.*, vol. 30, no. 2, pp. 763–772, Mar. 2015.

[12] D. Wang *et al.*, "A demand response and battery storage coordination algorithm for providing microgrid tie-line smoothing services," *IEEE Trans. Sustain. Energy*, vol. 5, no. 2, pp. 476–486, Jan. 2014.

[13] O. Erdinç, A. Taşcıkaraoğlu, N.G. Paterakis, Y. Eren, and J. P. S. Catalão, "End-user comfort oriented day-ahead planning for responsive residential HVAC demand aggregation considering weather forecasts," *IEEE Trans. Smart Grid*, vol. 8, no. 1, pp. 353–361, Jan. 2017.

[14] D. Wang, K. Meng, X. Gao, J. Qiu, L. L. Lai, and Z. Y. Dong, "Coordinated dispatch of virtual energy storage systems in LV grids for voltage regulation," *IEEE Trans. Ind. Informat.*, vol. 14, no. 6, pp. 2452–2462, Jun. 2018.

[15] Q. Wang, C. Lei, Y. Li, T. Wang, C. Wang, and N. Zhou, "A reactive power optimization model of high voltage distribution network considering DLC cycle control of air-conditioning loads," *Proc. CSEE*, vol. 38, no. 6, pp. 1684–1694, Mar. 2018.

[16] H. W. Qazi and D. Flynn, "Synergetic frequency response from multiple flexible loads," *Elect. Power Syst. Res*., vol. 145, pp. 185–196, Jan. 2017.
[17] J. Wang, H. Zhang, and Y. Zhou, "Intelligent under frequency and under voltage load shedding method based on the active participation of smart appliances," *IEEE Trans. Smart Grid*, vol. 8, no. 1, pp. 353–361, Jan. 2017.
[18] N. Lu and Y. Zhang, "Design considerations of a centralized load controller using thermostatically controlled appliances for continuous regulation reserves," *IEEE Trans. Smart Grid*, vol. 4, no. 2, pp. 914–921, Dec. 2013.
[19] Y. Zhang and N. Lu, "Parameter selection for a centralized thermostatically controlled appliances load controller used for intra-hour load balancing," *IEEE Trans. Smart Grid*, vol. 4, no. 4, pp. 2100–2108, May 2013.
[20] M. Aunedi, P. Kountouriotis, J. Calderon, D. Angeli, and G. Strbac, "Economic and environmental benefits of dynamic demand in providing frequency regulation," *IEEE Trans. Smart Grid*, vol. 4, no. 4, pp. 2036–2048, Dec. 2013.
[21] V. Trovato, F. Teng, and G. Strbac, "Role and benefits of flexible thermostatically controlled loads in future low-carbon systems," *IEEE Trans. Smart Grid*, vol. 9, no. 5, pp. 5067–5079, Sep. 2018.
[22] J. Kondoh, N. Lu, and D. J. Hammerstrom, "An evaluation of the water heater load potential for providing regulation service," *IEEE Trans. Power Syst.*, vol. 26, no. 3, pp. 1309–1316, Aug. 2011.
[23] H. Hao, T. Middelkoop, P. Barooah, and S. Meyn, "How demand response from commercial buildings will provide the regulation needs of the grid," in *Proc. 50th Annu. Allerton Conf. Commun. Control Comput.*, Monticello, IL, USA, Oct. 2012, pp. 1908–1913.
[24] H. Hao, A. Kowli, Y. Lin, P. Barooah, and S. Meyn, "Ancillary service for the grid via control of commercial building HVAC systems," in *Proc. Amer. Control Conf.*, Washington, DC, USA, Jun. 2013, pp. 467–472.
[25] Y. Lin, P. Barooah, S. Meyn, and T. Middelkoop, "Experimental evaluation of frequency regulation from commercial HVAC system," *IEEE Trans. Smart Grid*, vol. 6, no. 2, pp. 776–783, Dec. 2015.
[26] Y. Lin, P. Barooah, and S. Meyn, "Low-frequency power grid ancillary services from commercial building HVAC systems," in *Proc. IEEE Int. Conf. Smart Grid Commun.*, Vancouver, BC, Canada, Oct. 2013, pp. 169–174.
[27] G. Goddard, J. Klose, and S. Backhaus, "Model development and identification for fast demand response in commercial HVAC systems," *IEEE Trans. Smart Grid*, vol. 5, no. 4, pp. 2084–2092, Jul. 2014.
[28] P. Zhao, G. P. Henze, S. Plamp, and V. J. Cushing, "Evaluation of commercial building HVAC systems as frequency regulation providers," *Energy Build.*, vol. 67, pp. 225–235, Dec. 2013.
[29] I. Beil, I. Hiskens, and S. Backhaus, "Frequency regulation from commercial building HVAC demand response," *Proc. IEEE*, vol. 104, no. 4, pp. 745–757, Feb. 2016.
[30] M. Cheng *et al.*, "Power system frequency response from the control of bitumen tanks," *IEEE Trans. Power Syst.*, vol. 31, no. 3, pp. 1769–1778, May 2016.
[31] M. Cheng, J. Wu, S. Galsworthy, N. Gargov, W. Hung, and Y. Zhou, "Performance of industrial melting pots in the provision of dynamic frequency response in the Great Britain power system," *Appl. Energy*, vol. 201, pp. 245–256, Sep. 2017.
[32] *Mandatory Frequency Response (MFR)—Overview*, Nat. Grid plc, Jun. 2018. [Online]. Available: https://www.nationalgrid.com/uk/electricity/balancing-services/frequency-response-services/mandatory-response-services
[33] M. Cheng, J. Wu, S. Galsworthy, N. Jenkins, and W. Hung, "Availability of load to provide frequency response in the Great Britain power system," in *Proc. 18th Power Syst. Comput. Conf.*, Wroclaw, Poland, Aug. 2014, pp. 1–7.
[34] *Historic Frequency Data*, Nat. Grid plc, Jul. 2018. [Online]. Available: https://www.nationalgrid.com/uk/electricity/balancing-services/frequency-response-services/historic-frequency-data
[35] *Case Studies*, Open Energi, Oct. 2018. [Online]. Available: http://www.openenergi.com/case-studies/

Yue Zhou (M'13) received the B.S., M.S., and Ph.D. degrees in electrical engineering from Tianjin University, Tianjin, China, in 2011, 2016, and 2016, respectively.

He is currently a Postdoctoral Research Associate with the School of Engineering, Cardiff University, Cardiff, U.K. His research interests include demand response, frequency response, smart home energy management, optimization and blockchain technology.

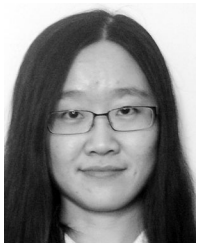

Meng Cheng received the B.Sc. degree in electrical and electronic engineering from Cardiff University, Cardiff, U.K., and North China Electric Power University, Beijing, China, in 2011, and the Ph.D. degree in electrical and electronic engineering from Cardiff University in 2015.

From 2015 to 2017, she was a Postdoctoral Research Associate with Cardiff University. She is currently a Senior Consultant with ABB (China) Ltd., Beijing. Her main research interests include smart grid and demand response.

Jianzhong Wu (M'04) received the B.S., M.S., and Ph.D. degrees in electrical engineering from Tianjin University, Tianjin, China, in 1999, 2002, and 2004, respectively.

From 2004 to 2006, he was a Postdoctoral Researcher with Tianjin University. From 2006 to 2008, he was a Research Fellow with the University of Manchester, U.K. He joined Cardiff University, Cardiff, U.K., in June 2008 (Lecturer 2008; Senior Lecturer 2013; Reader 2014; Professor 2015). He is currently a Professor of multivector energy systems and the Head of the Department of Electrical and Electronic Engineering, Cardiff University. He is a Subject Editor of applied energy. He is the Director of Applied Energy UNiLAB on Synergies between Energy Networks. He is a Co-Director of Supergen Hub on Energy Networks, and a Co-Principal Investigator of £24.5 m FLEXIS project. His research interests include energy infrastructure and smart grid.